The Hemes of *Escherichia coli* Nitrate Reductase A (NarGHI): Potentiometric Effects of Inhibitor Binding to NarI†

Richard A. Rothery,‡,§ Francis Blasco,§,|| Axel Magalon,⊥ Marcel Asso,@ and Joel H. Weiner*,‡

Medical Research Council of Canada Group in the Molecular Biology of Membrane Proteins, Department of Biochemistry, 474 Medical Sciences Building, University of Alberta, Edmonton, Alberta T6G 2H7, Canada, Laboratoire de Chimie Bactérienne, CNRS, 31 chemin Joseph Aiguier, 13402 Marseille Cedex 9, France, Lehrstuhl für Mikrobiologie der Universität München, Maria-Ward-Strasse 1a, 80638 München, Germany, and Laboratoire de Bioénergétique et Ingénierie des Protéines, CNRS, 31 chemin Joseph Aiguier, 13402 Marseille Cedex 9, France

Received March 8, 1999; Revised Manuscript Received June 30, 1999

ABSTRACT: We have potentiometrically characterized the two hemes of *Escherichia coli* nitrate reductase A (NarGHI) using EPR and optical spectroscopy. NarGHI contains two hemes, a low-potential heme b_L ($E_{m,7}$ = 20 mV; g_z = 3.36) and a high-potential heme b_H ($E_{m,7}$ = 120 mV; g_z = 3.76). Potentiometric analyses of the g_z features of the heme EPR spectra indicate that the $E_{m,7}$ values of both hemes are sensitive to the menaquinol analogue 2-*n*-heptyl-4-hydroxyquinoline *N*-oxide (HOQNO). This inhibitor causes a potential-inversion of the two hemes (for heme b_L, $E_{m,7}$ = 120 mV; for heme b_H, $E_{m,7}$ = 60 mV). This effect is corroborated by optical spectroscopy of a heme b_H-deficient mutant (NarGHI^{H56R}) in which the heme b_L undergoes a $\Delta E_{m,7}$ of 70 mV in the presence of HOQNO. Another potent inhibitor of NarGHI, stigmatellin, elicits a moderate heme b_L $\Delta E_{m,7}$ of 30 mV, but has no detectable effect on heme b_H. No effect is elicited by either inhibitor on the line shape or the $E_{m,7}$ values of the [3Fe-4S] cluster coordinated by NarH. When NarI is expressed in the absence of NarGH [NarI(ΔGH)], two hemes are detected in potentiometric titrations with $E_{m,7}$ values of 37 mV (heme b_L; g_z = 3.15) and −178 mV (heme b_H; g_z = 2.92), suggesting that heme b_H may be exposed to the aqueous milieu in the absence of NarGH. The identity of these hemes was confirmed by recording EPR spectra of NarI(ΔGH)^{H56R}. HOQNO binding titrations followed by fluorescence spectroscopy suggest that in both NarGHI and NarI(ΔGH), this inhibitor binds to a single high-affinity site with a K_d of approximately 0.2 μM. These data support a functional model for NarGHI in which a single dissociable quinol binding site is associated with heme b_L and is located toward the periplasmic side of NarI.

Escherichia coli, when grown anaerobically with nitrate as the respiratory oxidant, develops a respiratory chain terminated by a membrane-bound quinol:nitrate oxidoreductase (NarGHI)[1] (*1*−*3*). This enzyme is a heterotrimeric complex [Fe-S] molybdoenzyme comprising a molybdenum cofactor-containing catalytic subunit (NarG, 139 kDa), an [Fe-S] cluster-containing electron-transfer subunit (NarH, 58 kDa), and a heme-containing membrane anchor subunit (NarI, 26 kDa). NarG and NarH comprise a cytoplasmically localized membrane extrinsic catalytic dimer (NarGH) anchored to the membrane by NarI. NarGHI is an excellent example of a family of bacterial [Fe-S] molybdoenzymes, which includes *E. coli* DMSO reductase [DmsABC (*4*)], formate dehydrogenase N [FdnGHI (*5*)], and *Wolinella succinogenes* polysulfide reductase [PsrABC (*6*)]. The nitrate-reducing active site of NarGHI appears to comprise a Mo-bisMGD cofactor in which the Mo center has $E_{m,8}$ values of approximately 95 [Mo(IV/V)] and 195 mV [Mo(V/VI)] (*7*−*9*). The NarH [Fe-S] clusters have been extensively characterized using a combination of site-directed mutagenesis and EPR (*8*, *10*−*12*), and comprise one [3Fe-4S] cluster and three [4Fe-4S] clusters. In membranes enriched with NarGHI, the [3Fe-4S] cluster appears to exist as two potentiometrically distinct subpopulations with very similar EPR spectra: a major (70%) component with an $E_{m,8}$ of 180 mV and a minor (30%) component with an $E_{m,8}$ of 100 mV (*9*). The three [4Fe-4S] clusters have $E_{m,8}$ values of 130, −55, and −400 mV ([4Fe-4S] clusters) (*9*). On the basis of their nitrate oxidizability, roles for the two hemes of NarI, the

† This work was funded by a grant from the Medical Research Council of Canada to J.H.W. (PG11440) and by the Centre National de la Recherche Scientifique. F.B. was supported by a travel grant from the Alberta Heritage Foundation for Medical Research. A.M. was supported by a NATO Collaborative Research Grant awarded to J.H.W.

* To whom correspondence should be addressed: Medical Research Council of Canada Group in the Molecular Biology of Membrane Proteins, Department of Biochemistry, 474 Medical Sciences Building, University of Alberta, Edmonton, AB T6G 2H7. Telephone: (780) 492-2761. Fax: (780) 492-0886.

‡ University of Alberta.

§ The first two authors contributed equally to this paper.

|| CNRS.

⊥ Lehrstuhl für Mikrobiologie der Universität München.

@ Laboratoire de Bioénergétique et Ingénierie des Protéines.

[1] Abbreviations: DmsABC, DMSO reductase; FrdABCD, fumarate reductase; HALS, highly anisotropic low-spin; HOQNO, 2-*n*-heptyl-4-hydroxyquinoline *N*-oxide; Mo-bisMGD, molybdo-bis(molybdopterin guanine dinucleotide); NarGHI, nitrate reductase holoenzyme; NarGH, nitrate reductase soluble dimer; NarI(ΔGH), nitrate reductase cytochrome *b* subunit in the absence of NarGH; SdhCAB, *Bacillus subtilis* succinate dehydrogenase; SdhC(ΔAB), *B. subtilis* succinate dehydrogenase cytochrome *b* subunit in the absence of SdhAB.

10.1021/bi990533o CCC: $18.00
Published on Web 09/09/1999

[3Fe-4S] cluster, and the highest-potential [4Fe-4S] cluster have been proposed in electron transfer from quinol to nitrate (*12*−*15*). The relationship between the hemes of NarI and the role of this subunit in quinol binding and oxidation are not yet fully understood (*13*, *14*, *16*).

One of the factors that distinguishes NarGHI and FdnGHI from other members of the family of bacterial [Fe-S] molybdoenzymes is the presence of heme in their membrane anchor subunits (*16*). While the hemes of FdnI remain relatively poorly characterized, significant progress has been made in determining the EPR properties, heme ligation (*14*), kinetic properties, and sensitivity to inhibitors (*13*) of the two hemes of NarI. This 225-amino acid residue protein has five transmembrane helices (TM1−TM5) in which the N-terminus is believed to be periplasmically localized (*16*). Its two hemes were originally reported to have E_m values of 122 and 17 mV in redox titrations followed by optical spectroscopy (*17*). We obtained preliminary EPR data which suggested that one of the hemes does indeed have an E_m of approximately 120 mV (heme b_H) and that the other has an E_m that is approximately 100 mV lower (heme b_L) (*14*). Both hemes exhibit highly anisotropic low-spin (HALS) EPR spectra (*18*) that are consistent with a near-perpendicular orientation of the planes of the imidazole heme iron ligands. Heme b_L has a g_z of 3.36 and heme b_H a g_z of 3.76 (*14*), and there is a significant similarity between the overall composite spectrum and that of the cytochrome bc_1 complex [e.g., the cytochrome *b* spectra reported by Salerno (*19*)]. Analyses of site-directed mutants of NarGHI place heme b_L toward the periplasmic side of the NarI (coordinated by His-66 and His-187) and heme b_H toward the cytoplasmic side (coordinated by His-56 and His-205). In common with the cytochrome *b* subunit of the cytochrome bc_1 complex (*20*), the two hemes are coordinated by His residues in two transmembrane helices (TM2 and TM5 in NarI). This contrasts with what is found in other bacterial hydrophobic diheme cytochromes *b* which have ligands provided typically by four transmembrane helices, for example, in the membrane anchor subunit (SdhC) of *Bacillus subtilis* succinate dehydrogenase (SdhCAB) (*21*, *22*).

In both SdhCAB and the cytochrome bc_1 complex, the two hemes have high (heme b_H) and low (heme b_L) E_m values. In both cases, quinol and quinone binding site inhibitors have been shown to alter the E_m values of one or both hemes (*23*, *24*). In the recently determined structure of the cytochrome bc_1 complex, it has been demonstrated that the sites of inhibitor binding overlap with the proposed sites of ubiquinone and ubiquinol binding (*20*, *25*). Both HOQNO and stigmatellin are potent inhibitors of the quinol:nitrate oxidoreductase activity of NarGHI which also affect the EPR line shape and optical properties of heme b_L (*13*, *15*). It has been proposed that these inhibitors bind to a quinol binding site (the Q_p site) in the vicinity of heme b_L (*13*). Intriguingly, they also appear to elicit significant inhibition of nitrate-dependent heme oxidation (*13*). A study of the effects of these inhibitors on the redox potentiometry of the hemes of NarGHI may provide important insights into their relationship with the quinol binding site(s) of the enzyme.

When NarI is expressed and assembled into the cytoplasmic membrane in the absence of NarGH [NarI(ΔGH)], its low-spin heme EPR spectrum is dramatically altered compared to that of the holoenzyme (*13*, *15*). The EPR spectrum of NarI(ΔGH) exhibits two g_z features that can be attributed to low-spin ferric heme, one at 3.15 and another at 2.92. On the basis of its inhibitor-sensitivity, we have assigned the $g_z = 3.15$ feature to heme b_L (*13*). However, the identity of the heme giving rise to the $g_z = 2.92$ feature remains uncertain. The observation of a $g_z = 2.92$ feature may correlate with an almost parallel orientation of the imidazole heme iron ligands (*18*, *26*). In the case of NarI(ΔGH), this feature arises either from a significantly modified or "relaxed" form of heme b_H or from a subpopulation of heme b_L (*13*). In the latter case, NarI(ΔGH) would only contain a single heme. This uncertainty arises because the optical spectrum of NarI(ΔGH) is similar to the spectrum of $NarGHI^{H56R}$, which lacks heme b_H (*14*). It would be interesting to unequivocally identify the hemes of NarI(ΔGH) giving rise to the $g_z = 3.15$ and $g_z = 2.92$ spectral features and to determine their $E_{m,7}$ values.

The fluorescence properties of HOQNO (*27*, *28*) have recently been used to quantify the number of dissociable inhibitor binding sites within two other *E. coli* anaerobic reductases, DmsABC (*29*) and fumarate reductase (FrdABCD) (*30*, *31*). In both cases, binding with very high affinity ($K_d \leq 7$ nM) occurs at a single dissociable site that may be equivalent to the dissociable menaquinol (MQH_2) binding site. It has recently been proposed on the basis of steady-state kinetics experiments that both duroquinol (a ubiquinol analogue) and menadiol (a MQH_2 analogue) bind at two sites within the NarGHI complex (*32*). It has also been proposed that there is a tightly bound menaquinone-9 associated with the membrane extrinsic NarGH dimer (*33*) that may be involved in electron transfer from the hemes of NarI to the [3Fe-4S] cluster of NarH (*15*). Studies of the effect of the inhibitors HOQNO and stigmatellin on nitrate-dependent heme reoxidation suggest that there may be a second quinol or inhibitor binding site [the Q_{nr} site (*13*)] located between heme b_h and the [3Fe-4S] cluster of NarH. However, in another study in which the hydroxylated naphthoquinone lapachol was utilized (a MQH_2 analogue), no steady-state kinetic evidence was found for the binding of this substrate at more than one dissociable site (*34*). One characteristic of NarGHI which makes the hypothesis that there are two dissociable quinol binding sites attractive is the ability of the enzyme to use both MQH_2 and ubiquinol as reducing substrates (*12*, *32*, *35*, *36*). It is possible that there are two sites demonstrating "cross-inhibition" (*32*), one which is specific for ubiquinol and the other which is specific for MQH_2. However, it is also possible that there is one site that is able to accommodate both ubiquinol and MQH_2. It would therefore be interesting to determine the number of HOQNO binding sites in NarGHI using the HOQNO fluorescence technique.

In this paper, we have studied the electrochemistry of the hemes of NarI using both EPR and optical spectroscopy. We have investigated the effect of the absence of either heme on the $E_{m,7}$ of the other in two site-directed mutants of NarGHI (NarI-H56R and NarI-H66Y mutants) and have investigated the redox potentiometry of NarI(ΔGH). In addition, we have quantitated the number of high-affinity HOQNO binding sites within NarGHI and have investigated the effect of the absence of either heme and the absence of the NarGH dimer on inhibitor binding.

MATERIALS AND METHODS

Bacterial Strains and Plasmids. E. coli LCB2048 [*thi-1, thr-1, leu-6, lacY1, supE44, rpsL175* Δnar25(*narG-narH*) Δ(*nar′U-narZ′*), Ω (Spc^R), Km^R] (*37*) was used as the host for all the experiments described herein. Wild-type, NarI-H56R, and NarI-H66Y NarGHI were expressed from pVA700, pVA700-H56R, and pVA700-H66Y, respectively (*14*). NarI(ΔGH) was expressed from plasmid pCD7 (*14*). NarI(ΔGH)^{H56R} was expressed from plasmid pCD7-H56R which was generated using the Expand High Fidelity PCR System (Boehringer). pVA700, pCD7, and pCD7-H56R bear their respective genes under the control of the *tac* promoter.

Growth of Cells and Preparation of Membrane Vesicles Enriched with Wild-Type and Mutant NarGHI. Cells were grown microaerobically in 2 L batch cultures of Terrific Broth (*38*) at 30 °C in the presence of 100 μg/mL streptomycin and ampicillin. A 10% innoculum was used, and NarGHI overexpression was achieved by addition of 0.2 mM isopropyl-1-thio-β-D-galactopyranoside (IPTG). Following addition of the innoculum and IPTG, cells were grown overnight while they were gently shaken at 30 °C. Cells were harvested by centrifugation and washed in 100 mM MOPS and 5 mM EDTA (pH7). Crude membranes were prepared as previously described (*39*). These were resuspended in buffer and layered on top of a 62% (w/v) sucrose step (made up in buffer). Following centrifugation at 40 000 rpm for 2 h, the floating band enriched with the cytoplasmic membrane fraction was removed, diluted in buffer, and subjected to a further centrifugation. Finally, to ensure complete removal of residual sucrose, the pellet was resuspended in buffer and recentrifuged. Membranes were then resuspended in buffer to a concentration of approximately 30 mg/mL, flash-frozen in liquid nitrogen, and stored at −70 °C until they were used. Membranes of LCB2048 containing no NarGHI were prepared as described above except that only streptomycin was present in the growth medium, no IPTG was used, and a 55% (w/v) sucrose step was used to isolate the inner membrane fraction.

Growth of Cells and Preparation of Membrane Vesicles Enriched with NarI(ΔGH) and NarI(ΔGH)^{H56R}. Cells (LCB2048/pCD7 or LCB2048/pCD7-H56R) were grown as described above, except that the temperature was 37 °C and the cultures were grown for 4 h rather than overnight. Membrane vesicles were prepared using the protocol outlined above using a 55% sucrose step to purify the cytoplasmic membrane fraction.

Redox Potentiometry Followed by EPR Spectroscopy. Redox titrations were carried out under argon at 25 °C in 100 mM MOPS and 5 mM EDTA (pH7.0) as previously described (*40*). The following redox mediators were used at a concentration of 50 μM: quinhydrone, 2,6-dichlorophenolindophenol, 1,2-naphthoquinone, toluylene blue, phenazine methosulfate, thionine, duroquinone, methylene blue, resorufin, indigo trisulfonate, indigo disulfonate, anthraquinone-2-sulfonic acid, phenosafranine, benzyl viologen, and methyl viologen. All samples were prepared in 3 mm internal diameter quartz EPR tubes, rapidly frozen in liquid nitrogen-chilled ethanol, and stored under liquid nitrogen until they were used. EPR spectra were recorded using a Bruker ESP300 spectrometer equipped with an Oxford Instruments ESR-900 flowing helium cryostat. EPR conditions were as described in the individual figure legends.

Redox Potentiometry Followed by Optical Spectroscopy. Redox titrations were carried out under argon in a total volume of approximately 2 mL of 100 mM MOPS (pH7.0) at a protein concentration of 9 mg/mL. The following mediator dyes were used at a concentration of 3 μM: 1,2-naphthoquinone, phenazine methosulfate, methylene blue, resorufin, and phenosafranine. Optical data were collected at 559 nm using a Kontron Uvikon 932 double-beam spectrophotometer equipped with a temperature-controlled cuvette holder and a magnetic stirrer. The redox potential of the cuvette was measured using a Metrohm combination (platinum/reference) microelectrode.

Fluorescence Quenching Assay of HOQNO Binding to NarGHI- and NarI-Enriched Membranes. Quenching of HOQNO fluorescence (*27*−*30*, *41*) was used to determine the concentration of dissociable high-affinity HOQNO sites in NarGHI and NarI(ΔGH). Fluorescence intensities were measured with an excitation wavelength of 341 nm and an emission wavelength of 479 nm using a Perkin-Elmer LS-50B luminescence spectrometer. All experiments were carried out at pH 7.0 in 100 mM MOPS and 5 mM EDTA. HOQNO was added to the fluorescence cuvette from a 0.1 mM stock ethanolic solution. A range of protein concentrations was used as indicated in the individual figure legends. The observed fluorescence (F_{obs}) was fitted to an equation describing ligand binding to a single site as described by Okun et al. (*28*, *41*):

$$F_{obs} = (f_{bound} - f_{free})(Q - \sqrt{Q^2 - n_s[E_{tot}][I_{tot}]}) + f_{free}[I_{tot}] \quad (1)$$

with

$$Q = {}^1/_2([I_{tot}] + K_d + n_s[E_{tot}]) \quad (2)$$

and

$$[I_{tot}] = [I_{bound}] + [I_{free}] \quad (3)$$

These equations are from ref *41*. f_{bound} and f_{free} are the specific fluorescences of the bound and free inhibitor, respectively. $[I_{tot}]$, $[I_{bound}]$, and $[I_{free}]$ are the concentrations of total, bound, and free inhibitor, respectively. $[E_{tot}]$ is the total concentration of enzyme. n_s is the number of binding sites. In the case of the studies reported by us herein and elsewhere (*29*−*31*), the fluorescence of bound HOQNO is assumed to be zero ($f_{bound} = 0$).

Protein Assays. Protein concentrations were assayed by the Lowry method, modified by the inclusion of 1% (w/v) sodium dodecyl sulfate in the incubation mixture to solubilize membrane proteins (*42*).

Polyacrylamide Gel Electrophoresis. Polyacrylamide (12.5%) gel electrophoresis was carried out using the Bio-Rad mini gel system and a discontinuous SDS buffer system (*43*). Gels were stained with Coomassie Blue, destained, and digitally scanned, and the protein bands corresponding to the NarGHI holoenzyme were quantified relative to the total amount of Coomassie Blue-stained protein using the public

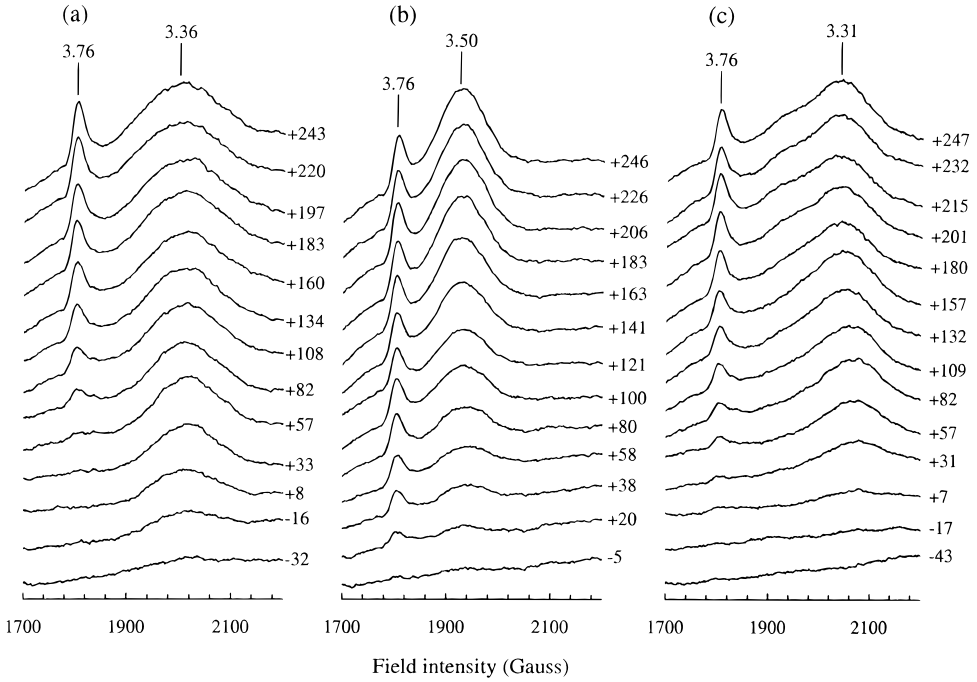

FIGURE 1: Effect of HOQNO and stigmatellin on potentiometric titrations of the hemes of NarGHI. (a) EPR spectra of redox-poised samples in the absence of inhibitors. (b) EPR spectra of redox-poised samples in the presence of 0.5 mM HOQNO. (c) EPR spectra of redox-poised samples in the presence of 0.3 mM stigmatellin. Samples were of cytoplasmic membranes enriched with NarGHI at a protein concentration of approximately 30 mg/mL in 100 mM MOPS and 5 mM EDTA (pH 7.0). Spectra were recorded under the following conditions: temperature, 12 K; microwave power, 100 mW at 9.47 GHz; and modulation amplitude, 19 G_{pp} at 100 kHz. For each spectrum, the E_h in millivolts is as indicated.

domain software package NIH Image, version 1.61 (developed at the National Institutes of Health).

RESULTS

Potentiometric Effects of HOQNO and Stigmatellin on the Two Hemes of NarGHI. Because HOQNO and stigmatellin have been previously demonstrated to be potent inhibitors of NarGHI (*13*, *36*), we determined their effects on the redox potentiometry of the two hemes of NarI. Figure 1a shows EPR spectra recorded at 12 K of redox-poised samples from a potentiometric titration of membranes enriched with NarGHI in the absence of HOQNO or stigmatellin. Noticeable in the fully oxidized spectrum (>200 mV) are the HALS features we have previously assigned to heme b_H ($g_z = 3.76$, low-field peak) and b_L ($g_z = 3.36$, high-field peak) (*13*, *14*). As the potential is decreased below approximately 200 mV, the intensity of the heme b_H signal begins to diminish, and below approximately 100 mV, the intensity of the heme b_L signal diminishes. Figure 1b shows equivalent spectra recorded in the presence of HOQNO. In this case, the position of the heme b_L g_z is shifted to 3.50 (*13*). Inspection of the spectra suggests that the hemes titrate with $E_{m,7}$ values that are closer together than those of the uninhibited enzyme (see below). In the presence of stigmatellin, the heme b_L g_z is shifted to approximately 3.31 (*13*), and again, the $E_{m,7}$ values appear to be closer together than those of uninhibited NarGHI (Figure 1c). At high potentials in the presence of stigmatellin, there appears to be some heterogeneity in the heme b_L g_z, with a minor component being present at approximately $g = 3.50$ (a shoulder on the low-field side of the $g = 3.31$ peak).

To obtain estimates of the intensities of the heme b_H and b_L g_z features in the presence and absence of inhibitors, it was necessary to partially eliminate errors due to the sloping baseline in this region of the spectrum [due to the adventitiously bound Fe(III) signal at $g = 4.3$]. To do this, the membranes used to generate the data in Figure 1 were prepared by sucrose step centrifugation to increase the specific concentration of NarGHI to approximately 46% of the total protein (see below). Second, the intensities of the features were determined by subtraction of a polynomial baseline fitted to the nonsignal portions of the spectra of Figure 1. In this way, it was possible to generate plots of signal intensity versus E_h. Figure 2a shows plots of the intensities of the heme b_H and heme b_L signals versus E_h. In agreement with previously reported values (*14*, *17*), the two hemes of NarI titrate with $E_{m,7}$ values of 120 (b_H) and 20 mV (b_L). In the presence of HOQNO, the potentials of the hemes are almost reversed (Figure 2b). In this case, heme b_H titrates with an $E_{m,7}$ of 60 mV, and heme b_L titrates with an $E_{m,7}$ of 120 mV, suggesting that HOQNO binding elicits conformational changes in the vicinity of both hemes. In the presence of stigmatellin (Figure 2c), heme b_H titrates with an $E_{m,7}$ of 120 mV, and heme b_L titrates with an $E_{m,7}$ of 50 mV. Thus, it is clear that HOQNO affects the redox properties of both hemes, whereas stigmatellin appears to affect only heme b_L.

To attempt to corroborate the effects of HOQNO shown in Figures 1 and 2, we carried out redox titrations followed by optical spectroscopy. Figure 3a shows optical redox titration data in the presence and absence of HOQNO. It is important to note that both hemes of NarI exhibit reduced α-band absorbance bands at approximately 560 nm at room temperature, precluding facile deconvolution of the spectra corresponding to hemes b_H and b_L (see Figure 1 of ref *14*). In the absence of HOQNO, the data of Figure 3a can be

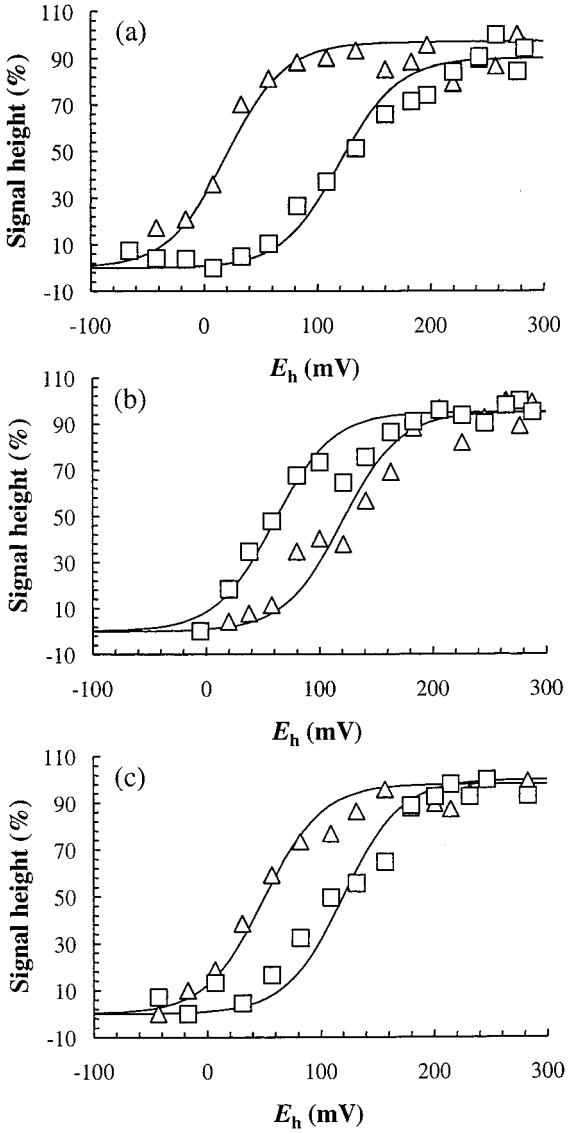

FIGURE 2: Effect of inhibitors on the NarI heme midpoint potentials determined by EPR: (a) no inhibitors, (b) 0.5 mM HOQNO, and (c) 0.3 mM stigmatellin and (□) heme b_H and (△) heme b_L. $E_{m,7}$ values were estimated as follows: (a) 120 (b_H) and 20 mV (b_L), (b) 60 (b_H) and 120 mV (b_L), and (c) 120 (b_H) and 50 mV (b_L). EPR spectra were recorded as described in the legend of Figure 1. Peak heights were determined after polynomial baseline subtraction using the OS9 computer of the ESP300 spectrometer system. The solid lines represent $n = 1$ fits to the Nernst equation.

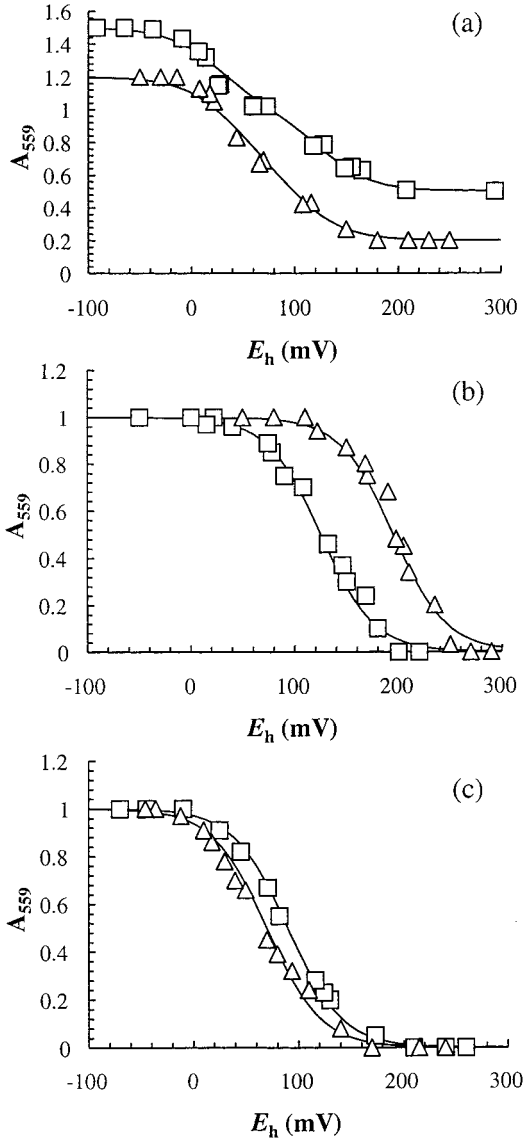

FIGURE 3: Optical redox titrations of the NarI hemes. (a) Wild-type NarGHI in the absence (□) and presence (△) of 0.5 mM HOQNO. Data were fitted to two components of equal absorbance with $E_{m,7}$ values of 125 and 28 mV (no HOQNO) and 100 and 40 mV (0.5 mM HOQNO). (b) NarGHI^{H56R} in the absence (□) and presence (△) of 0.5 mM HOQNO. Data were fitted to one component with an $E_{m,7}$ of 125 (no HOQNO) and 195 mV (0.5 mM HOQNO). (c) NarGHI^{H66Y} in the absence (□) and presence (△) of 0.5 mM HOQNO. Data were fitted to one component with an $E_{m,7}$ of 90 (no HOQNO) and 70 mV (0.5 mM HOQNO). Absolute absorbance values were normalized to a maximum of 1.0.

fitted to two components with $E_{m,7}$ values of 125 (b_H) and 28 mV (b_L), in good agreement with the data presented in Figure 2a. In the presence of HOQNO, the data can be fitted to two $E_{m,7}$ values of 100 and 40 mV. These data illustrate the advantage of the EPR method in determining inhibitor effects on the $E_{m,7}$ values of the hemes of NarI, as the redox state of two hemes with α-bands at 560 nm (but different g_z values) can easily be resolved by EPR but not by room-temperature optical spectroscopy.

To demonstrate, using optical spectroscopy, the large shift elicited on the heme b_L $E_{m,7}$ by HOQNO, we performed redox titrations on membranes enriched with NarGHI^{H56R}, a heme b_H deficient mutant (*14*) (Figure 3b). In the absence of HOQNO, the remaining heme of this mutant (heme b_L) titrates with an $E_{m,7}$ of 125 mV, indicating that the absence of heme b_H results in a significant modification of the environment of heme b_L which causes a $\Delta E_{m,7}$ of around 100 mV. In the presence of HOQNO, the $E_{m,7}$ is shifted to 195 mV, a $\Delta E_{m,7}$ of 70 mV which compares to the $\Delta E_{m,7}$ of 100 mV observed in redox titrations of the holoenzyme followed by EPR (Figure 2). The effect of HOQNO on a mutant lacking heme b_L was studied using the NarI-H66Y mutant. In this case, in the absence of HOQNO, heme b_H has an $E_{m,7}$ of 90 mV (Figure 3c), which suggests that, as in the case of the NarI-H56R mutant, there is a significant modification of the environment of the remaining heme caused by the absence of the other. In the presence of HOQNO, there is a modest shift in the $E_{m,7}$ of heme b_H to 70 mV, a $\Delta E_{m,7}$ of −20 mV. The $E_{m,7}$ values for the hemes of NarI and the effects of HOQNO are summarized in Table 1.

Table 1: Summary of Redox Potentiometry of the Hemes of NarI

	$E_{m,7}$ (mV)			
	without HOQNO		with HOQNO	
enzyme	EPR[a]	optical[b]	EPR	optical
NarGHI	120 (b_H)	125 (b_H)	60 (b_H)	40 (b_H)
	20 (b_L)	28 (b_L)	120 (b_L)	100 (b_L)
NarGHI^{H56R}	nd	125 (b_L)	nd[c]	195 (b_L)
NarGHI^{H66Y}	nd	90 (b_H)	nd	70 (b_H)
NarI(ΔGH)[d]	−178 (b_H)	nd	−172 (b_H)	nd
	37 (b_L)		72 (b_L)	

[a] $E_{m,7}$ values were obtained by plotting the intensities of the features that can be attributed to hemes b_H and b_L vs E_h. Data are representative of at least two independent redox titrations. Errors in the $E_{m,7}$ values are approximately ±10 mV. [b] $E_{m,7}$ values were obtained by plotting the absorbance at 560 nm vs E_h. Assignments of $E_{m,7}$ values to hemes b_H and b_L were based on comparison with EPR data (*13*, *14*). [c] Not determined. [d] NarI was overexpressed in the absence of NarGH from plasmid pCD7. Wild-type and mutant holoenzymes were expressed from wild-type and mutant plasmid pVA700 (*12*).

Level of Overexpression of NarGHI from pVA700. To interpret the potential effects of HOQNO and stigmatellin on the [3Fe-4S] cluster, it is necessary to estimate the EPR spectroscopic purity of NarGHI around $g = 2$ in LCB2048/pVA700 membranes. Figure 4A shows EPR spectra recorded at 12 K of ferricyanide-oxidized LCB2048 membranes containing no NarGHI [Figure 4A(i)] and overexpressed NarGHI [Figure 4A(ii)]. The intensity of the background [3Fe-4S] signal at $g = 2.02$ corresponds to approximately 15% of that of the signal in membranes containing overexpressed NarGHI. To confirm this, we subjected membranes from LCB2048 and LCB2048/pVA700 to SDS−PAGE analysis (Figure 4B). In the lane corresponding to membranes from LCB2048/pVA700, the intensity of the protein bands corresponding to the subunits of NarGHI comprises approximately 57% of the visible stained protein on the gel. This estimate of NarGHI content is consistent within experimental error with the amount detected by EPR spin quantitation of the NarH [3Fe-4S] cluster (see below; Table 2). Given that overexpression of NarGHI dilutes the species responsible for the background signal of Figure 4A(i), it is likely that the NarGHI [3Fe-4S] cluster accounts for ≥90% of the [3Fe-4S] EPR signal of oxidized LCB2048/pVA700 membranes.

Lack of an Effect of HOQNO or Stigmatellin on the EPR Line Shape or Redox Potentiometry of the NarH [3Fe-4S] Cluster. In two other terminal reductases of *E. coli*, DmsABC and FrdABCD, a significant effect is elicited by HOQNO on an engineered [3Fe-4S] cluster and an endogenous [3Fe-4S] cluster, respectively (*30*, *40*). Figure 4C shows EPR spectra of the oxidized (redox-poised) NarH [3Fe-4S] cluster in the absence of inhibitors [Figure 4C(i)] and in the presence of HOQNO [Figure 4C(ii)] or stigmatellin [Figure 4C(iii)]. It is clear from these spectra that no significant effects appear to be elicited by these inhibitors on the EPR line shape of the NarH [3Fe-4S] cluster. Potentiometric analyses of the [3Fe-4S] cluster followed by EPR suggest that in the absence of inhibitors, the cluster titrates with two $E_{m,7}$ values of 95 (30%) and 195 mV (70%) (data not shown), in agreement with our previous observations (*9*). No other [3Fe-4S] cluster subpopulations were detected throughout the range of E_h values that were studied. In the presence of 0.5 mM HOQNO, the potentials are 110 (30%) and 200 mV (70%).

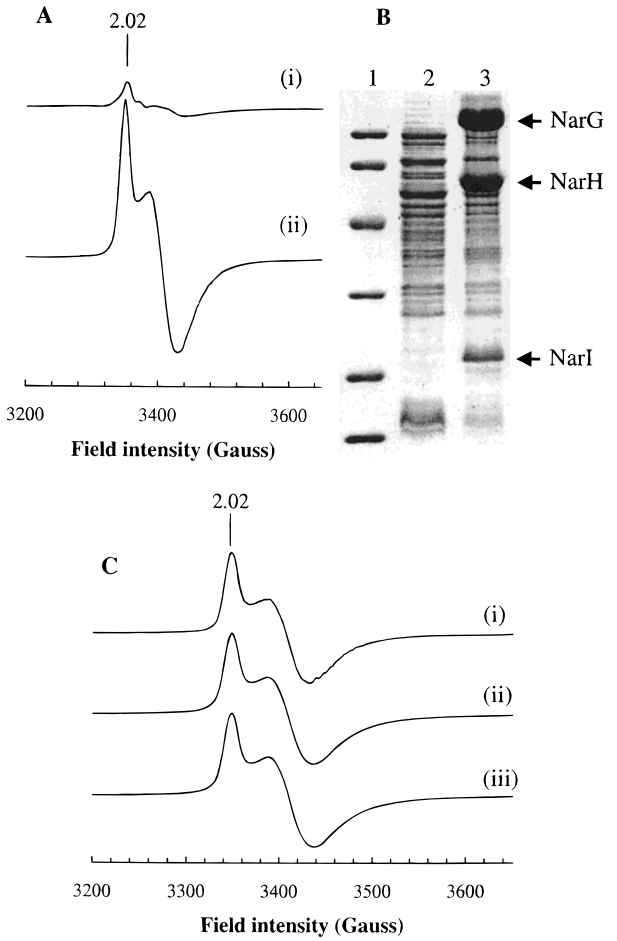

FIGURE 4: (A) EPR spectra of oxidized membranes from LCB2048 (i) and LCB2048/pVA700 (ii). EPR spectra were recorded at 12 K with a modulation amplitude of 10 G_{pp} at 100 kHz and a microwave power of 20 mW at a frequency of 9.47 GHz. Spectra were corrected for protein concentration to a nominal value of 30 mg/mL. Samples were oxidized with 0.2 mM potassium ferricyanide for 1 min prior to being frozen in liquid nitrogen. (B) Coomassie Blue-stained SDS−PAGE gel of isolated inner membranes from LBC2048 and LCB2048/pVA700: lane 1, low-molecular mass markers (Bio-Rad; phosphorylase b, 97.4 kDa; bovine serum albumin, 66.2 kDa; ovalbumin, 45 kDa; carbonic anhydrase, 31 kDa; soybean trypsin inhibitor, 21.5 kDa; and lysozyme, 14.4 kDa); lane 2, 45 μg of LCB2048 membrane protein; and lane 3, 45 μg of LCB2048/pVA700 membrane protein. The intensity of the bands corresponding to the subunits of NarGHI corresponds to approximately 57% by gel densitometry (approximately 2.6 nmol/mg of protein). (C) Effect of HOQNO and stigmatellin on the [3Fe-4S] cluster of NarGHI. EPR spectra of redox-poised membranes enriched with NarGHI at a protein concentration of approximately 30 mg/mL in the absence of inhibitors at an E_h of 248 mV (i), in the presence of 0.5 mM HOQNO at an E_h of 287 mV (ii), and in the presence of 0.3 mM stigmatellin at an E_h of 283 mV (iii). EPR conditions were as described for panel A.

Likewise, in the presence of 0.3 mM stigmatellin, these potentials are 105 (30%) and 200 mV (70%). We have previously shown that both the high- and low-potential subpopulations of the [3Fe-4S] cluster signal have the same line shape and arise from NarGHI (*9*). Thus, neither inhibitor appears to have a significant effect on the $E_{m,7}$ values of the NarH [3Fe-4S] cluster.

Assignment of the EPR Spectral Features of NarI(ΔGH). Figure 5A shows low-spin heme EPR spectra of membranes enriched with NarI(ΔGH) [Figure 5A(i)] and NarI(ΔGH)^{H56R} [Figure 5A(ii)]. The spectrum of NarI(ΔGH) is essentially

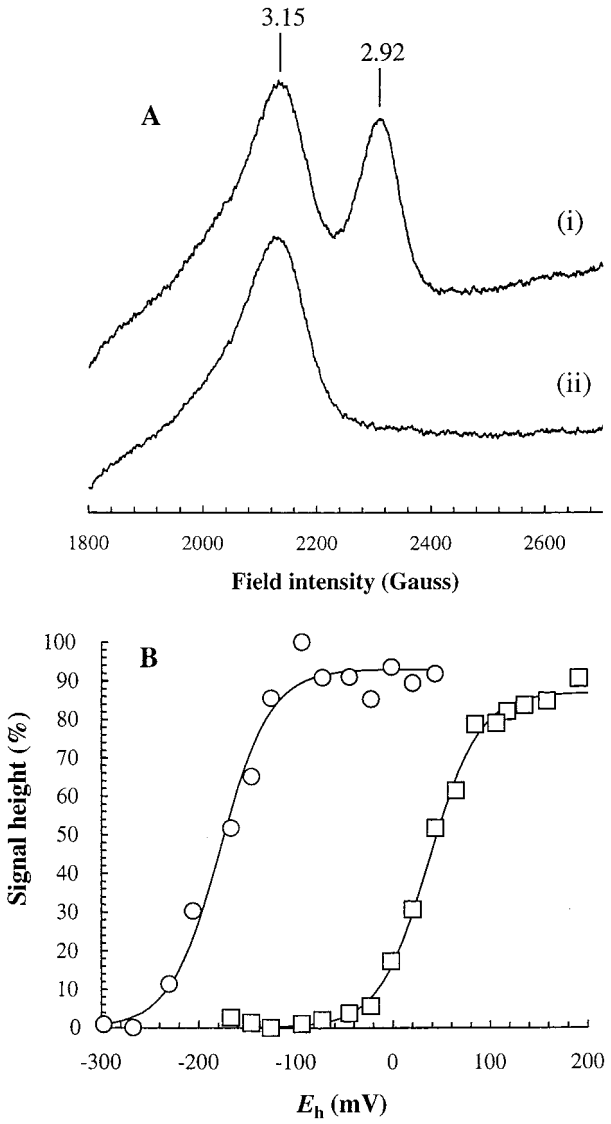

FIGURE 5: (A) EPR spectra of NarI(ΔGH) and NarI(ΔGH)^{H56R}. Spectra of (i) wild-type NarI(ΔGH) and (ii) H56R mutant NarI(ΔGH). EPR spectra were recorded under the conditions described in the legend of Figure 1 except the microwave power was 2 mW and three scans were accumulated. The spectra were normalized to a nominal protein concentration of 30 mg/mL. (B) Potentiometric titration of the hemes of wild-type NarI(ΔGH). Plots of the intensity of the $g = 3.15$ peak (□; $E_{m,7} = 37$ mV) and the $g = 2.92$ peak (○; $E_{m,7} = -178$ mV) of the NarI spectrum vs E_h. For each E_h, the intensity of the spectrum at $g = 3.03$ (the trough between the two peaks) was subtracted from the intensities at $g = 3.15$ and $g = 2.92$, respectively.

identical to that previously reported by us (*13*, *14*) with peaks at $g_z = 3.15$ (heme b_L, low-field peak) and $g_z = 2.92$ (high-field peak). On the basis of inhibitor-induced perturbations of the $g_z = 3.15$ peak, we have previously assigned this feature to heme b_L (*13*), whereas the assignment of the $g_z = 2.92$ feature remained uncertain. To resolve this issue, we recorded the low-spin EPR spectra of membranes enriched with NarI(ΔGH)^{H56R} [Figure 5A(ii)]. Clearly, mutagenesis of NarI-H56 results in the loss of the $g_z = 2.92$ peak of the spectrum, but has no detectable effect on the $g_z = 3.15$ peak. Given that NarI-H56 is a ligand to heme b_H in the NarGHI holoenzyme (*14*), we conclude that the $g_z = 2.92$ feature of the spectrum of NarI(ΔGH) arises from heme b_H and that the environment of this heme has been modified by the absence of the membrane extrinsic NarGH dimer (see the Discussion).

Potentiometric Analysis of NarI(ΔGH). Figure 5B shows plots of the intensities of the NarI(ΔGH) $g = 3.15$ and $g = 2.92$ peaks as a function of E_h in samples from a potentiometric titration. The $g_z = 3.15$ heme b_L peak titrates with an $E_{m,7}$ of 37 mV. In contrast, the $g_z = 2.92$ heme b_H peak titrates with an $E_{m,7}$ of −178 mV. This represents a $\Delta E_{m,7}$ of approximately −300 mV compared to the $E_{m,7}$ of this heme in the NarGHI holoenzyme (see the Discussion).

In the presence of HOQNO, the $g_z = 3.15$ feature is shifted to $g_z = 3.45$ (*13*) and its $E_{m,7}$ is shifted from approximately 37 to 72 mV, a $\Delta E_{m,7}$ of 35 mV (data not shown, Table 1). HOQNO has no detectable effect on either the position of the heme b_H g_z (*13*) or its $E_{m,7}$. Therefore, the absence of the NarGH dimer either appears to result in the loss of the conformational link between the two hemes of NarI or results in the loss of inhibitor binding in the vicinity of heme b_H (see the Discussion).

Fluorescence Quenching Assay of HOQNO Binding to Membranes Enriched with NarGHI, NarGHI^{H56R}, NarGHI^{H66Y}, and NarI(ΔGH). We have previously demonstrated that the fluorescence of HOQNO is quenched when it is bound to the MQH_2 binding sites of *E. coli* DmsABC (*29*) and FrdABCD (*30*, *31*). We used this phenomenon to estimate the number of high-affinity HOQNO binding sites within NarGHI. Figure 6a shows a series of HOQNO binding titrations for membranes enriched with NarGHI at a range of protein concentrations between approximately 0.2 and 0.8 mg/mL. In these titrations, there is an upward curvature of the plot of fluorescence versus HOQNO concentration. This curvature can be fitted to a K_d and a specific enzyme concentration as described in Materials and Methods. Membranes enriched with NarGHI contain 2.06 nmol of independent (i.e., noncooperative binding) HOQNO binding sites/mg of protein which have a K_d of 0.20 μM (Table 2). This compares with a NarGHI concentration based on that of the oxidized [3Fe-4S] cluster of 1.91 nmol/mg of protein (estimated by EPR spin quantitation), suggesting that there are approximately 1.08 HOQNO binding sites per NarGHI heterotrimer. In the heme b_H deficient mutant, NarGHI^{H56R} (Figure 6b), there are 2.05 nmol of independent HOQNO binding sites/mg of protein which have a K_d of approximately 0.18 μM. In this mutant, the [3Fe-4S] cluster EPR spectrum is modified and its intensity diminished (*14*), resulting in an estimated number of HOQNO binding sites per [3Fe-4S] cluster of 1.18 (Table 2). In the heme b_L deficient mutant, NarGHI^{H66Y} (Figure 6c), there is an almost undetectable upward curvature of the plots of fluorescence versus HOQNO concentration, indicating that inhibitor binding occurs with a K_d of approximately 1.0 μM. Because of the low curvature, the specific enzyme concentration used in the fits to the data was treated as invariant and was assumed to be 1.74 nmol/mg of protein, as estimated by EPR spin quantitation. Finally, HOQNO binds to NarI(ΔGH) with a K_d of 0.20 μM and an estimated specific concentration of sites of 5.13 nmol/mg of protein (data not shown, Table 2). In all the cases that were studied, the data can be fitted to a binding equation (*41*) (see Materials and Methods) describing noncooperative inhibitor binding to a single site that appears to be sensitive to the presence of heme b_L.

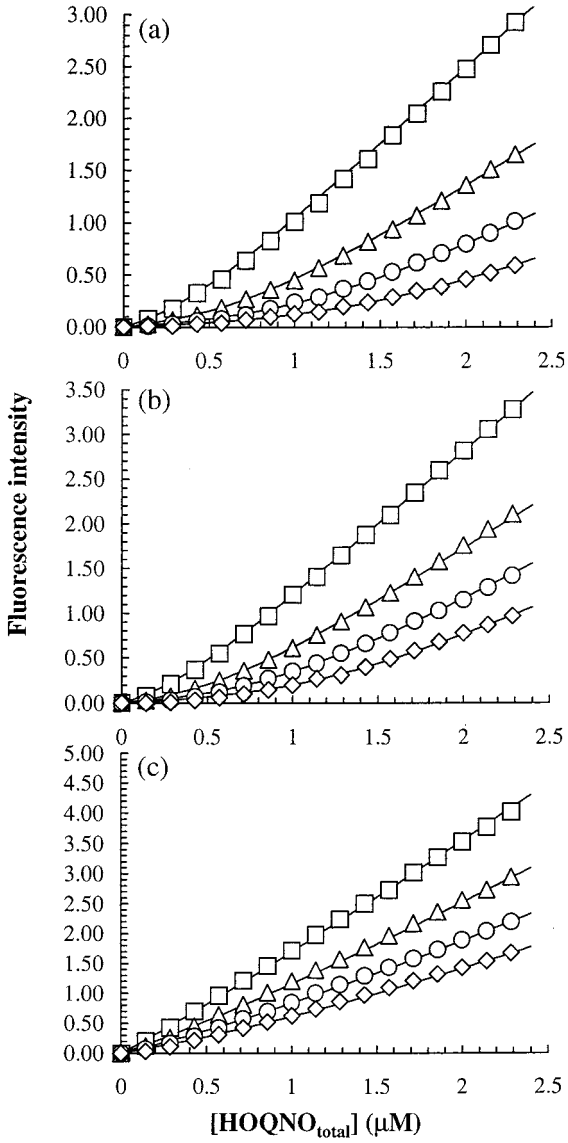

FIGURE 6: HOQNO binding titrations of membranes enriched with wild-type (a), NarI-H56R (b), and NarI-H66Y NarGHI (c). (a) For the wild-type, titrations were carried out at four protein concentrations: 0.19 (□), 0.39 (△), 0.58 (○), and 0.78 mg/mL (◇). Data were fitted to a K_d of 0.20 μM, one HOQNO binding site, and a specific enzyme concentration of 2.06 nmol/mg of protein (45.7% membrane protein). (b) NarGHI^{H56R}. Titrations were carried out at 0.16 (□), 0.33 (△), 0.49 (○), and 0.66 mg/mL protein (◇). Data were fitted to a K_d of 0.18 μM, one HOQNO binding site, and a specific enzyme concentration of 2.05 nmol/mg of protein (45.5% membrane protein). (c) NarGHI^{H66Y}. Titrations were carried out at the same protein concentrations as described for NarGHI^{H56R}. Data were fitted to a K_d of 1.0 μM and a specific enzyme concentration of 1.74 nmol/mg of protein (38.4% membrane protein). In this case, the specific enzyme concentration was derived from EPR spin quantitation of the NarH [3Fe-4S] cluster and was treated as invariant in the analysis.

Equivalency of HOQNO and Stigmatellin Binding Sites within NarGHI. Both HOQNO and stigmatellin are potent inhibitors of the quinol:nitrate oxidoreductase activity of NarGHI (*13*). To determine if stigmatellin binding blocks HOQNO binding to NarI, HOQNO binding titrations were carried out in the presence of 2.75 μM stigmatellin (Figure 7). In the absence of stigmatellin, there is a normal titration curve essentially identical to those of panels a and b of Figure 6. In the presence of stigmatellin, most of the curvature corresponding to HOQNO binding to NarGHI is eliminated.

Table 2: HOQNO Binding to Wild-Type and Mutant NarGHI

preparation	K_d (μM)	[Q sites] (nmol/mg of protein)	[3Fe-4S][a] (nmol/mg of protein)	HOQNO sites per enzyme[b]
NarGHI	0.20	2.06	1.91	1.08
NarGHI^{H56R}	0.18	2.05	1.74[c]	1.18
NarGHI^{H66Y}	1.00	1.74	1.74	1.00
NarI(ΔGH)	0.20	5.13	nd[d,e]	nd

[a] The [3Fe-4S] concentration was estimated by EPR spin quantitation of spectra of this cluster under nonsaturating conditions using a CuEDTA concentration standard (*51*). [b] Based on the assumption that each NarGHI holoenzyme contains a single [3Fe-4S] cluster. [c] The [3Fe-4S] cluster spectral line shape in NarGHI^{H56R} is modified and its intensity diminished (*14*). [d] Not determined. [e] The [3Fe-4S] cluster is absent from pCD7-overexpressed NarI; therefore, it was not possible to estimate the concentration of NarI by this method.

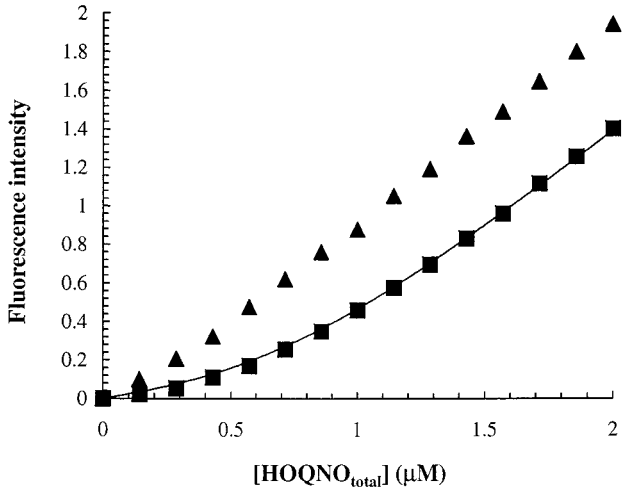

FIGURE 7: Effect of stigmatellin on HOQNO binding to NarGHI. (■) Membranes (0.39 mg/mL) enriched with wild-type NarGHI were titrated with HOQNO as described in the legend of Figure 6. (▲) Wild-type NarGHI (0.39 mg/mL) was titrated in the presence of 2.75 μM stigmatellin.

Data similar to those presented in Figure 7 were obtained in all cases where high-affinity HOQNO binding was detected [i.e., in NarI(ΔGH) and NarGHI^{H56R}, data not shown].

DISCUSSION

We have demonstrated the effects of two potent inhibitors of NarGHI on the redox potentiometry of the two hemes of the NarI subunit. HOQNO has a significant effect on both hemes, whereas stigmatellin appears to have only a significant effect on heme b_L. In the case of stigmatellin, the results are consistent with inhibitor binding at a site associated with heme b_L. This is in agreement with our previous studies on the effect of this inhibitor on the EPR line shape of this heme and the lack of effect on the line shape of heme b_H (*13*). In the case of HOQNO, the EPR line shape of heme b_L is affected (*13*), and the $E_{m,7}$ values of the hemes are inverted. This effect is consistent with a number of possibilities. (i) HOQNO binds to a site in the vicinity of heme b_L, and the conformational change elicited on this heme is propagated to heme b_H via movements of one or more of the transmembrane helices. (ii) HOQNO binds at two sites, one associated with heme b_L and another associated with heme b_H. This explanation is consistent with previous data suggesting that there may be a second quinol binding site located between

heme b_H and the [3Fe-4S] cluster of NarH (*13*, *15*). However, HOQNO binding titrations followed by fluorescence spectroscopy appear to indicate that high-affinity binding at a single site is dependent on the presence of heme b_L. If there is indeed a Q site between heme b_H and the [3Fe-4S] cluster [the Q_{nr} site (*13*)], then its affinity for HOQNO must be at least 1 order magnitude lower than that of the site associated with heme b_L (the Q_p site).

The effect of HOQNO on the redox properties of the two hemes bears interesting comparison with its effect on the hemes of *B. subtilis* SdhCAB (*23*). In SdhCAB, the two hemes of SdhC have high (heme b_H, 65 mV) and low (heme b_L, −96 mV) E_m values (*23*). The E_m of heme b_L is sensitive to HOQNO, and this results in a ΔE_m of approximately −57 mV (*23*); on the other hand, there is no effect on the E_m of heme b_H. The coordination of the two hemes of SdhC is such that four transmembrane helices provide His ligands (*21*). In the case of NarI, the two hemes are coordinated by TM2 and TM5 (*14*, *16*). This would allow for the propagation of conformational effects via these helices. It is surprising that the $\Delta E_{m,7}$ elicited by HOQNO on heme b_L of SdhCAB has a sign that is the opposite of that observed in NarGHI. This may reflect a significant difference between the quinol binding site of NarGHI and that of SdhCAB, which may be a result of the preference of the latter enzyme for MQ over UQ as the quinone substrate (*44*).

In the cytochrome bc_1 complex, the two hemes have $E_{m,7}$ values of approximately 92 (b_H) and −31 mV (b_L) (*24*). In this case, both hemes are associated with quinol binding sites, the Q_n and Q_p sites, respectively. The Q_p site is also associated with the Rieske [2Fe-2S] cluster (*20*). Stigmatellin has been shown to elicit a large ΔE_m of >200 mV on the Rieske [2Fe-2S] cluster (*45*, *46*), but has little effect on either of the hemes *b* (*24*). Other inhibitors, such as antimycin A, alter the E_m values of both hemes. As is the case for NarI (*14*), the two hemes of the cytochrome bc_1 complex are coordinated between two transmembrane helices (*20*). There is also a striking similarity between EPR spectra recorded of the hemes of NarI and those of the two cytochrome bc_1 hemes *b* (*19*). However, in the case of the bc_1 complex, the more anisotropic heme signal corresponds to heme b_L and the less anisotropic signal corresponds to heme b_H. Thus, it is unlikely that there is a reliable relationship between the anisotropy of the HALS spectrum and the observed $E_{m,7}$ values of the corresponding hemes. Another similarity between NarI and the bc_1 complex is the effect of losing heme b_H on the $E_{m,7}$ of heme b_L. In both cases (Figure 3 and Table 1) (*47*), there is a large positive ΔE_m for heme b_L in the absence of heme b_H.

The effect of stigmatellin on the redox properties of heme b_L of NarI does not appear to be propagated to heme b_H. In contrast to HOQNO, stigmatellin decreases the g_z of heme b_L (*13*), suggesting that this inhibitor may cause a decrease in the angle between the planes of the histidine ligand imidazoles, whereas HOQNO may cause an increase in this angle. It is therefore possible that the nature of the conformational change elicited by stigmatellin is sufficiently different from that elicited by HOQNO for it not to be propagated to heme b_H. We do not favor the alternative explanation that HOQNO, but not stigmatellin, binds to two sites within NarI, one associated with heme b_L and the other associated with heme b_H, for the following reasons. (i) HOQNO binding titrations (Figure 6 and Table 2) indicate the presence of only one high-affinity binding site for this inhibitor. Any additional site would have to have a K_d in excess of approximately 1 μM, beyond the sensitivity of the fluorescence assay used herein. (ii) We have previously demonstrated that both HOQNO and stigmatellin inhibit nitrate-dependent heme reoxidation, with the latter inhibitor being the more potent one (*13*). On this basis, it would be expected that stigmatellin would be more likely than HOQNO to elicit effects on the environment of heme b_H.

HOQNO binding to *E. coli* FrdABCD causes a significant change in the EPR line shape of the FR3 [3Fe-4S] cluster (*30*). For *E. coli* DmsABC, a similar line shape change was elicited on the EPR spectrum of a [3Fe-4S] cluster engineered into the DmsB subunit (*40*). In the structure of FrdABCD, an HOQNO-sensitive Q site is located approximately 11 Å from the FR3 [3Fe-4S] cluster (*48*). It has previously been proposed that in NarGHI there may be an additional inhibitor binding site (the Q_{nr} site) located between the heme b_H of NarI and the [3Fe-4S] cluster of NarH (*13*, *15*). The studies reported herein do not support this hypothesis. (i) No detectable line shape change of the [3Fe-4S] cluster is elicited by either HOQNO or stigmatellin (Figure 4B). (ii) No significant changes in the redox properties of the [3Fe-4S] cluster are elicited by these two inhibitors. (iii) High-affinity HOQNO binding is not observed in the absence of heme b_L. (iv) HOQNO binding appears to be unaffected by the absence of NarGH. These results suggest that there is no dissociable high-affinity inhibitor binding site located between heme b_H and the [3Fe-4S] cluster. However, it has been reported that there is a tightly bound menaquinone associated with the NarGH dimer (*33*), and we recently reported the observation of a semiquinone radical species that may be localized at this site during enzyme turnover (*15*). Thus, the fact that we have generated no data supporting the presence of a quinol site between heme b_H and the [3Fe-4S] cluster in the studies reported herein does not exclude the possibility that this site is present, but not dissociable or has a low affinity for HQONO. If the Q_{nr} site does exist and is dissociable, it would be difficult to reconcile its presence with the observed bioenergetics of electron-transport chains terminated by NarGHI (*49*). If this were the case, oxidation of quinol at the Q_{nr} site would likely result in the dissipation of the transmembrane proton electrochemical potential, in disagreement with the established bioenergetics of NarGHI (*49*). To assess the possible presence of a nondissociable Q_{nr} site, further studies with an *E. coli* mutant defective in MQH_2 biosynthesis (a *men*$^-$ mutant) aimed at determining if there is a nondissociable quinol binding site within NarGHI are in progress.

Redox titrations of membranes enriched with NarI(ΔGH) indicate that the inhibitor-sensitive g_z peak at 3.15 (heme b_L) titrates with an $E_{m,7}$ of 37 mV, whereas the inhibitor-insensitive g_z peak at 2.92 (heme b_H) titrates with an $E_{m,7}$ of −178 mV (Figure 5 and Table 1). EPR studies of NarI(ΔGH)^{H56R} confirm the above assignment (Figure 5). Thus, the g_z of heme b_H shifts from 3.76 to 2.92 in the absence of the NarGH dimer. Such a shift can be explained by a "relaxation" of the planes of the His imidazoles from a near-perpendicular orientation (resulting in a HALS spectrum) to a near-parallel orientation (resulting in a g_z at 2.92) (*13*, *18*, *26*). These observations suggest that heme b_H is

located close to the NarI−NarGH interface and that the apparent shift in the $E_{m,7}$ of heme b_H from 120 to −178 mV in NarI(ΔGH) may be caused by its exposure to the aqueous milieu. A similar phenomenon has been observed in chloroplast cytochrome b_{559} which results in a ΔE_m of approximately −300 mV upon exposure of the heme (*50*). We have previously shown that the loss of heme b_H (in NarGHI^{H56R}) results in a perturbation of the NarH [3Fe-4S] cluster EPR spectrum (*14*). Taken together, these observations suggest that heme b_H is located not only close to the NarI−NarGH interface but also close to the [3Fe-4S] cluster of NarH. This is consistent with electron transfer proceeding from heme b_L to heme b_H and then to the [3Fe-4S] cluster of NarH.

We have previously demonstrated that high-affinity HOQNO binding occurs at a single site in both *E. coli* DmsABC and FrdABCD (*29*−*31*). Although HOQNO binding to NarGHI occurs with a lower affinity than binding to DmsABC or FrdABCD (a K_d of approximately 0.2 μM compared to ≤7 nM), we were able to use the HOQNO fluorescence titration method to estimate the number of high-affinity inhibitor binding sites in NarGHI. It is clear that in all cases where inhibitor binding can be detected by EPR, binding of a single HOQNO per NarGHI could be detected by the fluorescence titration method. Binding of HOQNO appears to be blocked in the presence of stigmatellin (Figure 7) which has previously been demonstrated to be a more potent inhibitor of NarGHI than HOQNO (*13*). This suggests either that high-affinity binding of the two inhibitors either occurs at the same site within NarI or that there are two inhibitor-specific sites that are in close proximity and display cross-inhibition (*32*). Further studies of site-directed mutants of NarI will be necessary to distinguish between these possibilities.

Overall, we have determined the $E_{m,7}$ values of the hemes of NarI and the effects of the menaquinol analogue inhibitors HOQNO and stigmatellin. We have also demonstrated the effect of the loss of either heme on the redox properties of the remaining one, and the possibility that the absence of the NarGH dimer in NarI(ΔGH) may expose heme b_H to the aqueous milieu. In addition, by using fluorescence spectroscopy, we have shown that high-affinity HOQNO binding is heme b_L-dependent. These data support a model for quinol binding and oxidation by NarGHI in which a single dissociable binding site (Q_P) is located close to heme b_L toward the periplasmic side of NarI. Electrons derived from quinol oxidation at this site pass through heme b_L to heme b_H which is located toward the cytoplasmic side of NarI, very close to the NarI−NarGH interface. No evidence was found for inhibitor binding at a site (*13*) located between heme b_H and the [3Fe-4S] cluster of NarH. These results represent an important step in understanding quinol binding and oxidation by NarGHI.

ACKNOWLEDGMENT

We thank Chantal Frixon for technical assistance and Danielle Lemesle-Meunier for helpful discussions.

REFERENCES

1. Blasco, F., Iobbi, C., Giordano, G., Chippaux, M., and Bonnefoy, V. (1989) *Mol. Gen. Genet. 218*, 249−256.
2. Blasco, F., Pommier, J., Augier, V., Chippaux, M., and Giordano, G. (1992) *Mol. Microbiol. 6*, 221−230.
3. Berks, B. C., Ferguson, S. J., Moir, J. W. B., and Richardson, D. J. (1995) *Biochim. Biophys. Acta 1232*, 97−123.
4. Weiner, J. H., Rothery, R. A., Sambasivarao, D., and Trieber, C. A. (1992) *Biochim. Biophys. Acta 1102*, 1−18.
5. Berg, B. L., Li, J., Heider, J., and Stewart, V. (1991) *J. Biol. Chem. 266*, 22380−22385.
6. Krafft, T., Bokranz, M., Klimmeck, O., Schröder, I., Fahrenholz, F., Kojro, E., and Kröger, A. (1992) *Eur. J. Biochem. 206*, 5456−5463.
7. Magalon, A., Asso, M., Guigliarelli, B., Rothery, R. A., Bertrand, P., Giordano, G., and Blasco, F. (1998) *Biochemistry 37*, 7363−7370.
8. Guigliarelli, B., Asso, M., More, C., Augier, V., Blasco, F., Pommier, J., Giordano, G., and Bertrand, P. (1992) *Eur. J. Biochem. 207*, 61−68.
9. Rothery, R. A., Magalon, A., Giordano, G., Guigliarelli, B., Blasco, F., and Weiner, J. H. (1998) *J. Biol. Chem. 273*, 7462−7469.
10. Augier, V., Guigliarelli, B., Asso, M., Bertrand, P., Frixon, C., Giordano, G., Chippaux, M., and Blasco, F. (1993) *Biochemistry 32*, 2013−2023.
11. Augier, V., Asso, M., Guigliarelli, B., More, C., Bertrand, P., Santini, C., Blasco, F., Chippaux, M., and Giordano, G. (1993) *Biochemistry 32*, 5099−5108.
12. Guigliarelli, B., Magalon, A., Asso, M., Bertrand, P., Frixon, C., Giordano, G., and Blasco, F. (1996) *Biochemistry 35*, 4828−4836.
13. Magalon, A., Rothery, R. A., Lemesle-Meunier, D., Frixon, C., Weiner, J. H., and Blasco, F. (1998) *J. Biol. Chem. 273*, 10851−10856.
14. Magalon, A., Lemesle-Meunier, D., Rothery, R. A., Frixon, C., Weiner, J. H., and Blasco, F. (1997) *J. Biol. Chem. 272*, 25652−25658.
15. Magalon, A., Rothery, R. A., Giordano, G., Blasco, F., and Weiner, J. H. (1997) *J. Bacteriol. 179*, 5037−5045.
16. Berks, B. C., Page, M. D., Richardson, D. J., Reilly, A., Cavill, A., Outen, F., and Ferguson, S. J. (1995) *Mol. Microbiol. 15*, 319−331.
17. Hacket, N. R., and Bragg, P. D. (1982) *FEMS Microbiol. Lett. 13*, 213−217.
18. Walker, F. A., Huynh, B. H., Scheidt, W. R., and Osvath, S. R. (1986) *J. Am. Chem. Soc. 108*, 5288−5296.
19. Salerno, J. C. (1984) *J. Biol. Chem. 259*, 2331−2336.
20. Xia, D., Yu, C., Kim, H., Xia, J., Kachurin, A. M., Zhang, L., Yu, L., and Deisenhofer, J. (1997) *Science 277*, 60−66.
21. Hägerhäll, C., and Herderstedt, L. (1996) *FEBS Lett. 389*, 25−31.
22. Hägerhäll, C. (1997) *Biochim. Biophys. Acta 1320*, 107−141.
23. Smirnova, I. A., Hägerhäll, C., Konstantinov, A. A., and Hederstedt, L. (1995) *FEBS Lett. 359*, 23−26.
24. Howell, N., and Robertson, D. E. (1993) *Biochemistry 32*, 11162−11172.
25. Kim, H., Xia, D., Yu, C. A., Xia, J. Z., Kachurin, A. M., Zhang, L., Yu, L., and Deisenhofer, J. (1998) *Proc. Natl. Acad. Sci. U.S.A. 95*, 8026−8033.
26. Dou, Y., Admiraal, S. J., Ikeda-Saito, M., Krzywda, S., Wilkinson, A. J., Li, T., Olson, J. S., Prince, R. C., Pickering, I. J., and George, G. N. (1995) *J. Biol. Chem. 270*, 15993−16001.
27. van Ark, G., and Berden, J. A. (1977) *Biochim. Biophys. Acta 459*, 119−137.
28. Brandt, U., and von Jagow, G. (1991) *Eur. J. Biochem. 195*, 163−170.
29. Zhao, Z., and Weiner, J. H. (1998) *J. Biol. Chem. 273*, 20758−20763.
30. Rothery, R. A., and Weiner, J. H. (1998) *Eur. J. Biochem. 254*, 588−595.
31. Zhao, Z., Rothery, R. A., and Weiner, J. H. (1999) *Eur. J. Biochem. 260*, 50−56.
32. Giordani, R., Buc, J., Cornish-Bowden, A., and Cárdenas, M. L. (1997) *Eur. J. Biochem. 250*, 567−577.

33. Brito, F., DeMoss, J. A., and Dubourdieu, M. (1995) *J. Bacteriol. 177*, 3728−3735.
34. Rothery, R. A., Chatterjee, I., Kiema, G., McDermott, M. T., and Weiner, J. H. (1998) *Biochem. J. 332*, 35−41.
35. Wallace, B. J., and Young, I. G. (1977) *Biochim. Biophys. Acta 461*, 84−100.
36. Morpeth, F. F., and Boxer, D. H. (1985) *Biochemistry 24*, 40−46.
37. Blasco, F., Nunzi, F., Pommier, J., Brasseur, R., Chippaux, M., and Giordano, G. (1992) *Mol. Microbiol. 6*, 209−219.
38. Sambrook, J., Fritsch, E. F., and Maniatis, T. (1989) *Molecular Cloning: A Laboratory Manual*, 2nd ed., Cold Spring Harbor Laboratory Press, Cold Spring Harbor, NY.
39. Rothery, R. A., and Weiner, J. H. (1991) *Biochemistry 30*, 8296−8305.
40. Rothery, R. A., and Weiner, J. H. (1996) *Biochemistry 35*, 3247−3257.
41. Okun, J. G., Lümmen, P., and Brandt, U. (1999) *J. Biol. Chem. 274*, 2626−2630.
42. Markwell, M. A. D., Haas, S. M., Bieber, L. L., and Tolbert, N. E. (1978) *Anal. Biochem. 87*, 206−210.
43. Laemmli, U. K. (1970) *Nature 227*, 680−685.
44. Lemma, E., Unden, G., and Kröger, A. (1990) *Arch. Microbiol. 155*, 62−67.
45. von Jagow, G., and Ohnishi, T. (1985) *FEBS Lett. 185*, 311−315.
46. Liebl, U., Sled, V., Brasseur, G., Ohnishi, T., and Daldal, F. (1997) *Biochemistry 36*, 11675−11684.
47. Yun, C., Crofts, A. R., and Gennis, R. B. (1991) *Biochemistry 30*, 6747−6754.
48. Iverson, T. M., Luna-Chavez, C., Cecchini, G., and Rees, D. C. (1999) *Science 284*, 1961−1966.
49. Jones, W. R., Lamont, A., and Garland, P. B. (1980) *Biochem. J. 190*, 79−94.
50. Krishtalik, L. I., Tae, G. S., Cherepanov, D. A., and Cramer, W. A. (1993) *Biophys. J. 65*, 184−195.
51. Paulsen, K. E., Stankovich, M. T., and Orville, A. M. (1993) *Methods Enzymol. 227*, 396−411.

BI990533O